communications earth & environment

Article

https://doi.org/10.1038/s43247-024-01318-6

Polystyrene-degrading bacteria in the gut microbiome of marine benthic polychaetes support enhanced digestion of plastic fragments

Check for updates

Sufang Zhao[1,2], Renju Liu[1,3], Shiwei Lv[1,3], Benjuan Zhang[1,4], Juan Wang[1] & Zongze Shao[1,2,3,4]

Polystyrene foam, which is used as a buoyant material in mariculture, is a common constituent of marine plastic debris. Here, we conduct analyses on polystyrene foam debris collected on the east coast of Xiamen Island, China, and associated plastic-burrowing clamworms. We apply interferometry, mass spectrometry and microscopy to polystyrene foam fragments excreted by the benthic clamworms (*Perinereis vancaurica*). We find evidence of polystyrene digestion and degradation during passage of the clamworm gut leading to the formation and accumulation of microplastics, with a mean diameter of 0.6 ± 0.2 mm. 16S rRNA gene sequence analysis of clamworm intestines indicated diverse bacterial gut microbiome, dominated by *Acinetobacter* and *Ruegeria* bacteria. Further characterization confirmed that polystyrene was degraded by representative gut isolates of *Acinetobacter johnsonii*, *Brevibacterium casei*, and *Ruegeria arenilitoris*. During a 30-day incubation, we observed a very slight decrease in polystyrene weight, changes in chemical group and thermal characteristic, and production of polystyrene metabolic intermediates. Our findings indicate that polystyrene-degrading bacteria in the gut microbiome of clamworms may influence plastic fragmentation and degradation in marine ecosystems.

Polystyrene (PS) is composed of styrene monomers and is widely used in packaging containers and construction materials. Approximately 390 million tons of plastic were manufactured in 2021, with 5.3% of it being PS, which is mostly produced in polystyrene foams, including expanded polystyrene (EPS) and extracted polystyrene (XPS)[1]. The low density, excellent buoyancy and waterproof properties of EPS have led to its adoption in aquaculture. Each year, a large amount of EPS, including items such as abandoned fishing gear, construction and packaging materials, flows through rivers into the sea and can float with currents to gather in plastic garbage patches in oceanic areas[2]. EPS is more likely than expanded polypropylene (EPP) and polyethylene (EPE) to fracture into small fragments owing to their soft texture and relative susceptibility to photolytic degradation during wind/water current-assisted transport[3]. Microplastics are considered to be plastic fragments that are larger than one micrometer and smaller than five millimeters in any dimension[4]. PS microplastics can now be detected on the surface of global oceans[4–6]. Based on conservative estimates, more than 300 million microplastic particles (mostly < 1 mm in size) may be released annually into oceans through mariculture alone[7,8]. The PS microplastics that spread across marine farms also tend to be taken up by corals, planktonic organisms, crustaceans, mollusks and other marine animals, which may result in microplastic bioaccumulation in various food chains[9,10].

Although plastic pollutants are widely distributed in marine environments, little is known about their fate in the ocean or about the process of generating microplastics in situ[11]. During our investigation of EPS-degrading marine bacteria, we observed that EPS pieces previously floating on the sea surface were attached to diverse marine invertebrates, such as bivalves (mussels) and crustaceans (crabs, barnacles). Furthermore, hole-

[1]Key Laboratory of Marine Genetic Resources and Southern Marine Science and Engineering Guangdong Laboratory (Zhuhai), Third Institute of Oceanography, Ministry of Natural Resources of China, Xiamen 361005, China. [2]School of Marine Science and Technology, Harbin Institute of Technology, Weihai 264209, China. [3]School of Environmental Science, Harbin Institute of Technology, Harbin 150090, China. [4]School of Fisheries and Life, Shanghai Ocean University, Shanghai 201306, China. e-mail: shaozz@163.com

Fig. 1 | EPS were uptake by *P. vancaurica* and fragmented into microplastics. a The exposure scene of *P. vancaurica*. **b** The EPS blocks collection phenomenon. **c**, **d** The EPS were ingested by *P. vancaurica*. **e** Microplastics in frass.

boring clamworms seemed to feed on white EPS and excrete brown debris, forming tunnels inside the EPS and leading to microplastic accumulation (Fig. 1). The gut microbes, digestive enzymes and enzymes in the saliva of this clamworm may play important roles in this process. However, to the best of our knowledge, marine polychaete-mediated plastic degradation has never been reported, although the chewing of PE and EPS by terrestrial insect larvae has been reported.

The first case of an EPS-chewing insect was the yellow mealworm (*Tenebrio molitor*), and the PS-degrading bacterium *Exiguobacterium* sp. YT2 was isolated from the gut of this insect[12,13]. Moreover, a PS-degrading *Acinetobacter* bacterium was isolated from the larvae of *Tribolium castaneum* (*Coleoptera; Tenebrionidae*), which were shown to ingest EPS[14]; *Enterococcus* was found in the gut of the EPS-feeding larvae of the greater wax moth *Galleria mellonella* and *Tenebrio obscurus* (*Coleoptera: Tenebrionidae*)[15,16]; these gut bacteria were shown to be involved in PS degradation in vitro based on validation experiments of pure culture, although their role in the degradation of EPS in situ remains to be further determined, as they are common facultative anaerobes dominating the gut of other invertebrates and numerous other animals, including fish and human beings[17,18].

Benthic invertebrates are key species in marine ecosystems and are often used as indicators of environmental pollution[19]. Normally, the benthic polychaetes of *Perinereis* inhabit marine surface sediments, and their life activities include burrowing, construction and maintenance of galleries, acting as bioturbators at the sediment–water interface, and in most cases, inducing enhanced organic matter mineralization. *Perinereis* specimens are divided into the head, trunk and tail, with a pair of warty feet and a bundle of bristles on each segment of the trunk. The clamworm was characterized as a tropical and subtropical species of *Perinereis vancaurica* (*Polychaeta: Nereididae*)[20], which is widely distributed in the East China Sea, the South China Sea and beaches in the Atlantic Ocean of North and South America. This study aimed to understand the contribution of EPS-eating clamworms to marine microplastic formation and the potential role of the gut microbiome in PS digestion. We characterized the gut microbiome and obtained pure cultures of the predominant members of the gut with PS-degrading potential. These results extend our knowledge concerning the roles of marine benthic polychaetes and their associated gut microbiome in plastic biodegradation processes.

Results and discussion

Identification of the clamworm based on phylogenetic relationships

Morphological features of the EPS-eating clamworm were identical to the polychaete invertebrate (Supplementary Fig. S2). To perform molecular characterization of the clamworm, the mitochondrial 16S rRNA and COI genes were amplified and phylogenetic trees were constructed[21–23]. The mitochondrial 16S rRNA analysis revealed that the clamworm was closely related to *P. vancaurica* (accession number NC_065095.1) with 99% sequence similarity. The COI gene sequence similarity between the clamworm and *P. vancaurica* (MT511719.1) was 94%. The phylogenetic tree based on the neighbor-joining (NJ) method generated with a comparison of the mitochondrial 16S rRNA gene sequences showed that the clamworm clustered with *P. vancaurica* (Supplementary Fig. S3).

Excreted EPS frass was fragmented and biodegraded by clamworms

Clamworm feeding on EPS causes fragmentation (Fig. 1). Under SEM, the surface of the PS microplastics in the frass was altered (Fig. 2). A large number of cavities were observed, whereas the pristine EPS was smooth (Fig. 2a). The cavities in the EPS microplastics may be caused by gut microbe-induced degradation, digestive enzymes and physical grinding in the intestinal tract, which in turn enables gut microbes to colonize a large area of the EPS surface (Supplementary Fig. S4). Stereomicroscopic observations and statistical analysis indicated that the EPS particles ranged in size from 0.3 to 1.3 mm (<5 mm), with an average size of 0.6 ± 0.2 mm (Fig. 2b, d). Light microscopic observation revealed that the EPS particles included nanoplastics (<1 μm) with a size distribution between 0.5 μm and 15 μm (Supplementary Fig. S5).

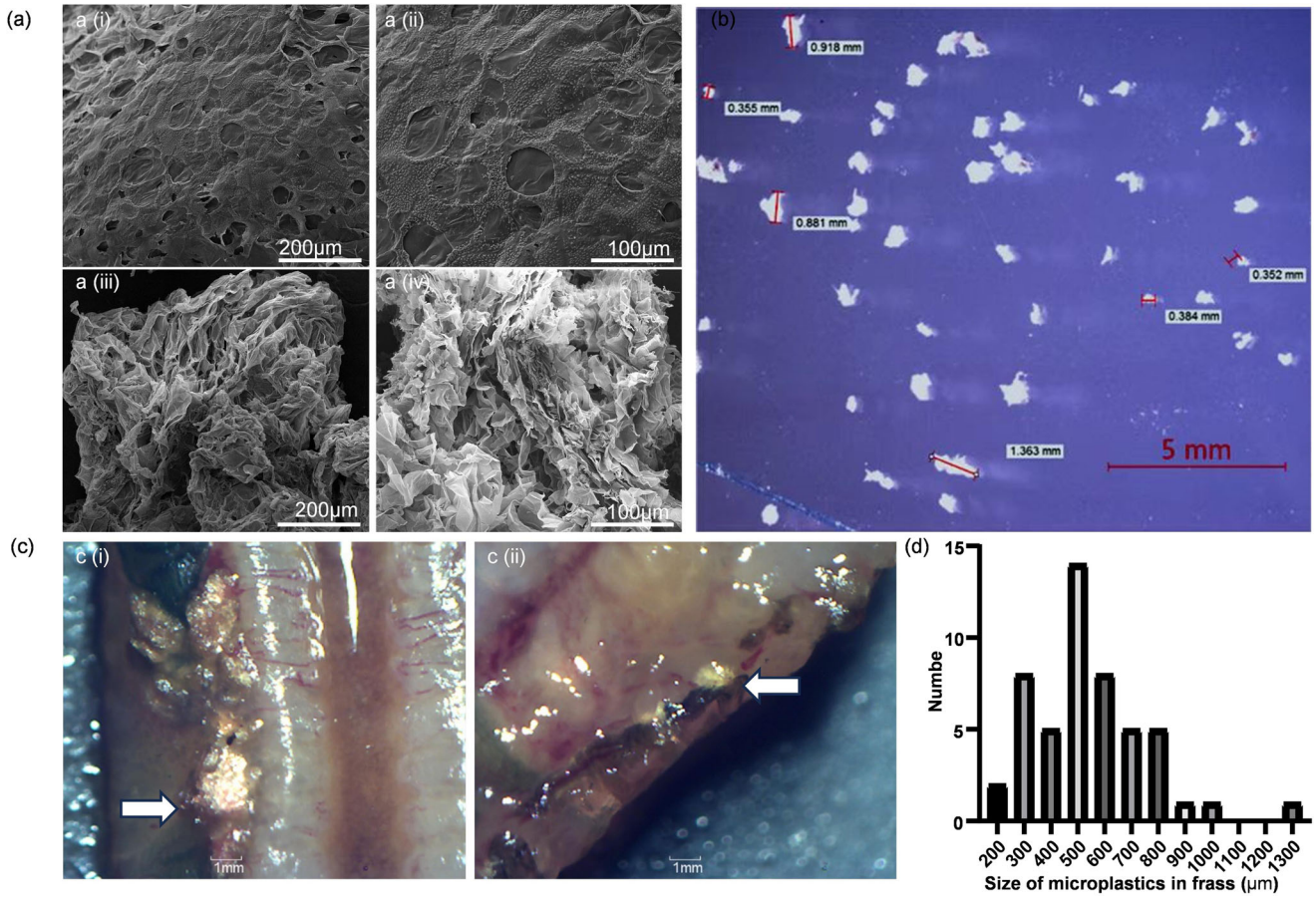

Fig. 2 | Depolymerization characteristics of EPS through the digestion of *P. vancaurica*. **a** SEM images showing surface modifications of EPS after biodegradation by the gut flora, ai–ii the EPS control and aiii–iv the biodegraded EPS by the clamworms. Bar, 200 μm or 100 μm. **b** The particle size of frass was observed by a stereo microscope after 2% SDS washing. **c** i-ii The EPS debris in the gut of clamworm was examined under a stereomicroscope. **d** The distribution of microplastic sizes of the extracted EPS frass.

Characterization of changes in EPS debris in the clamworm gut and excreted EPS frass

As shown in Fig. 2c and Supplementary Fig. S4, we found unexcreted EPS microplastics in the gut of clamworms and bacterial biofilms on the microplastic surface. EPS fragmentation by clamworms can increase the surface-to-volume ratio and promote degradation. GC–MS analysis indicated that long-chain fatty acids (FAAs) (peak 4; eicosanoic acid), benzene ring-containing substances (peak 1; benzoic acid,3,5-bis(1,1-dimethylethyl)-4-hydroxy) (peak 2; phenol,2,6-bis(1,1-dimethylethyl)-4-ethyl) and long-chain carboxylic acid esters (peak 3; hexadecanoic acid, methyl ester) were present in the gut of EPS-fed clamworm there exist (Fig. 3a). Benzene ring-containing substances (peak 5; 4-methyl-2,6-ditert-pentylphenol) were also present in the frass (Supplementary Table S2).

Currently, the PS metabolites of *T. molitor* and *G. mellonella* larvae have been reported. Tsochatzis et al. performed metabolite analysis of *Tenebrio molitor* larvae feeding on PS in different diets, and no degradation products were observed in the intestinal tissue or in the insect biomass, while in frass, PS monomers (styrene) and PS oligomers (dimers, trimers) were identified[13,24]. The degradation products of these oligomers include 2,4,6-triphenyl-1-hexene, 1,3,5-triphenylcyclohexane, 2,4-diphenyl-1-butene, 1,1-diphenyl cyclobutene, and trans-1,2-diphenycyclobutane[13]. The bioactive compounds of fatty acids (hexadecanoic acid, octadecanoic acid, tetradecanoic acid), amides (oleamide, tetradecanamide, hexadecanamide), and esters were identified in frass, in addition to several hydrocarbons[24]. Three bacteria (*Erwinia olea*, *Lactococcus lactis* and *Lactococcus garviae*) were found to be associated with PS biodegradation in the gut microflora of *T. molitor* under different PS-feeding strategies[13]. In another study, PS monomers (styrene, α-methylstyrene, acetophenone, α,α-dimethyl benzene methanol, 2,4-di-tert butyl phenol, and methyl-9,12-octadecadienoate), oligomers (2,4,6-triphenyl-1-hexene and 1,3,5-triphenylcyclohexane), bioactive molecules of fatty acids (myristic, palmitic, oleic, and undecanoic), esters (methyl linoleate, ethyl linoleate, and ethyl palmitate) and amides (tetradecanamide, hexadecanamide, and oleamide) were identified in the extract of freeze-dried homogenates from *T. molitor* larvae fed a single PS diet[25].

Wang et al. and Lou et al. identified PS degradation metabolites in *G. mellonella* larvae, and PS degradation products (styrene, phenyl acetate, 4-methylphenol, 2-hydroxyphenyl acetate, homoformate, 4-hydroxybenzaldehyde, 4-hydroxybenzoate, and derivatives of acetyl coenzyme A) were found in intestinal tissue[26]; FFAs (oleic acid, octadecanoic acid, and n-hexadecanoic acid) were identified in frass, and changes in the intestinal microbiome suggested that *Bacillus subtilis* and *Sarcocytophagus myristicaulis* were associated with the PS diet[16]. The presence of C = O- and C − O functional groups and FFAs are indicative of metabolic intermediates of plastic depolymerization and biodegradation in relation to the increase in enzymatic, biochemical and intestinal microbiota activities in the larval gut[24,25,27].

In our study, PS monomers, FFAs and esters were also identified in the gut of EPS-fed clamworms, and PS monomers were present in the frass; among which, Benzoic acid,3,5-bis(1,1-dimethylethyl)-4-hydroxy ($C_{15}H_{22}O_3$) and 4-methyl-2,6-ditert-pentylphenol ($C_{16}H_{26}O$) were structurally similar to 4-hydroxybenzoate ($C_7H_6O_3$) and 4-methylphenol (C_7H_8O) in PS metabolites of *G. mellonella*, respectively[26]. We speculated that 4-methylphenol–4-hydroxybenzaldehyde–4-hydroxybenzoate pathway could

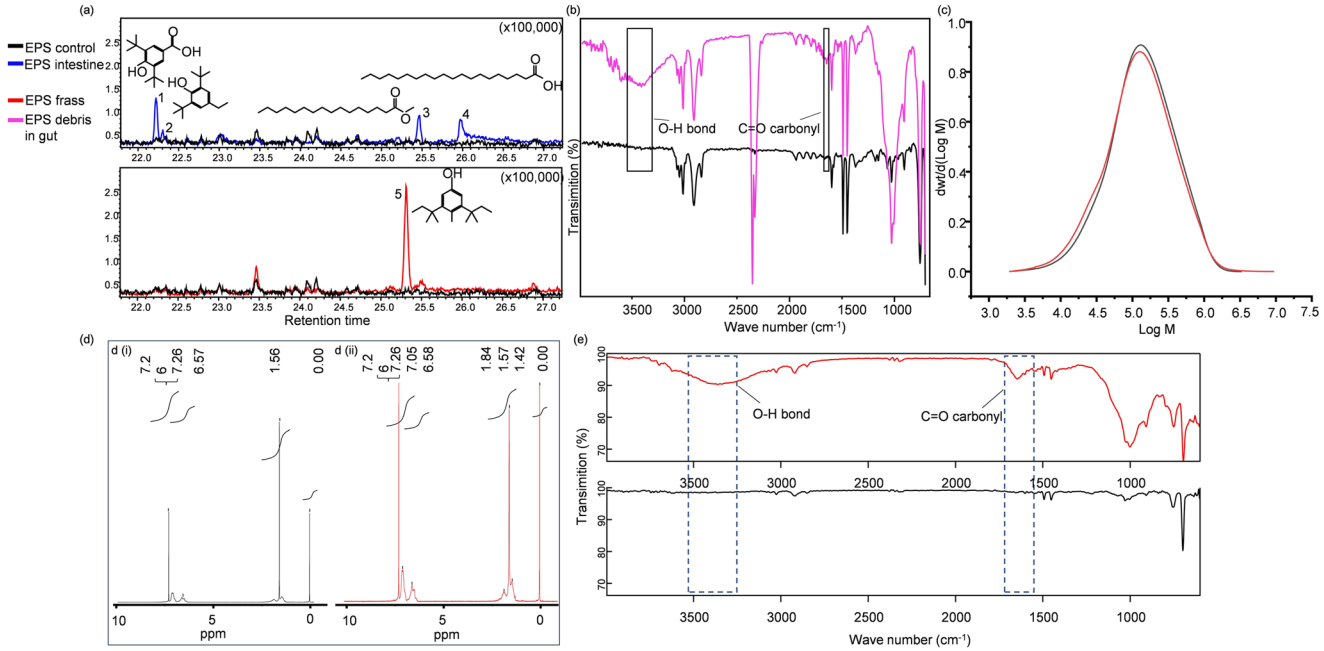

Fig. 3 | Characterization of depolymerization of EPS debris changes in the gut of clamworms and excreted EPS frass. a Gas chromatography-mass spectrometry (GC-MS) analysis of the plastic samples (EPS control), the intestine and fresh frass of EPS-eating clamworms. Compounds in figure: 1. Benzoic acid,3,5-bis(1,1-dimethylethyl)-4-hydroxy ($C_{15}H_{22}O_3$) 2. Phenol,2,6-bis(1,1-dimethylethyl)-4-ethyl) ($C_{16}H_{26}O$); 3.Hexadecanoic acid, methyl ester) ($C_{17}H_{34}O_2$); 4. Eicosanoic acid ($C_{20}H_{40}O_2$); 5. 4-methyl-2,6-ditert-pentylphenol ($C_{16}H_{26}O$). **b** μFTIR transmittance spectra of the EPS control and the EPS debris in the gut after digestion from 500-4000 cm^{-1}. **c** Molecular weight distribution shifts of EPS control and EPS frass. **d** (i-ii) ^{1}H NMR analysis of EPS frass showed it had a increase in the number of peaks in the aliphatic signal region (1-2 ppm) and aromatic portions (6-7 ppm) versus the EPS control. **e** FT-IR transmittance spectra of the EPS control and the extracted EPS frass from 500-4000 cm^{-1}.

be an alternative route for PS metabolism in the intestine of clamworms, which has been proposed for the gut of PS-fed *G. mellonella*[26].

Subsequent μFTIR observation of the EPS microplastics in the gut indicated enhanced -OH stretching absorption at approximately 3166-3790 cm^{-1} (HI = 11.9) and C = O stretching absorption at approximately 1616-1727 cm^{-1} (CI = 0.59) compared to those of the EPS control (HI = 0.02; CI = 0.33) (Fig. 3b). The results confirmed that the EPS ingested by the clamworms was partially biofragmented into MPs and biodegraded into various intermediates in the intestine. However, a percentage of the ingested EPS remained undigested in the form of microplastics, which were released into marine ecosystems.

The biodegradation of excreted EPS was examined using FTIR. The FTIR spectra of the digested frass excreted by the clamworms were compared with those of the EPS control. Consequently, the new enhanced functional group at 1670 cm^{-1} is attributed to the -C = O carbonyl group conjugated to aromatic rings, and the weak band at 3310 cm^{-1} is attributed to -OH bond stretching (Fig. 3e). The formation of new C = O and R-OH functional groups was similar to previous reports on the modification of egested frass from *Achatina fulica*, *T. molitor*, *Z. atratus*, *Plesiophthalmus davidis*, and *G. mellonella* during PS biodegradation[28–31]. Here, FTIR analysis indicated that EPS were biodegraded by clamworms or by microbes in the gut via oxidation.

GPC analysis confirmed that the Mw of EPS in frass decreased by 2.1% from 216.9 kDa to 212.3 kDa, while the Mn decreased by 12.5% from 73.5 kDa to 64.3 kDa when compared to that of the EPS control. Because Mn (12.5%) encompassed a wider range than Mw (2.1%), the molecular weight of the frass decreased, and depolymerization of the frass produced lower-molecular-weight fragments. A negative shift in the molecular weight distribution (MWD) indicated a shift in molecular weight towards a lower molecular weight after EPS passed through the clamworm gut, suggesting that more oligomeric products may be produced (Fig. 3c). The PDI of the EPS control (3.3) was greater than that of the frass control (2.95), suggesting a decrease in the molecular weight of the residual polymer and that the molecular weight reduction is more extensive for short-chain polymers than for long-chain polymers.

A similar depolymerization pattern of decreases in Mn and Mw and a shift in MWD towards lower molecular weights were observed during the biodegradation of PS by the larvae of *Z. atratus* (strain G larvae) (39.0% and 45.3%), *T. obscurus* (26.0% and 59.2%), *T. molitor* (11.7% and 29.8%), *P. davids* (4.1% and 3.3%) and *Acinetobacter* sp. AnTc-1 (13% and 25%) isolated from *T. castaneum*[14,15,29,32]. However, the pattern of PS depolymerization was broad, as was the pattern of PS degradation in *G. mellonlla* larvae, *A. fulica* and *Z. atratus* (Strain M), which resulted in an increase in Mn and Mw, as well as a shift in the MWD towards a higher molecular weight[16,28,32]. In our study, the decreases in the Mn and Mw of EPS consumed by *P. vancaurica* were lower than those of *T. molitor* and *T. obscurus* but were similar to the decreases in Mn and Mw and the negative shift in the MWD caused by *P. davidis*[15,29]. This indicated that *T. molitor* and *T. obscurus* might have superior PS depolymerization and biodegradation than *P. vancaurica*. Despite living inside the EPS block, clamworms may ingest organic matter attached to the EPS block surface or in seawater rather than feed with EPS as the sole carbon source, resulting in limited depolymerization of EPS, which corresponds to the limited weight loss caused by the isolates from the gut.

The chemical alteration of the frass was also confirmed by ^{1}H NMR analysis (Fig. 3d). Compared to the NMR spectrum of the EPS control, that of the frass showed 2 new peaks at 1-2 ppm, and 1 new peak appeared in the aromatic portions of the 6-7 ppm signal region[14]. The presence of additional peaks in the frass indicated that chemical structural changes occurred.

The physical (smaller particle size, increased surface-to-volume ratio) and chemical characteristics of microplastics from clamworm frass are different from those of uningested EPS, although the majority of ingested EPS are undigested by the clamworm as EPS frass found in clamworm holes in EPS blocks. A percentage of the microplastics retained in clamworm frass will eventually reach the ocean. These findings suggest that marine burrowers facilitate the generation of

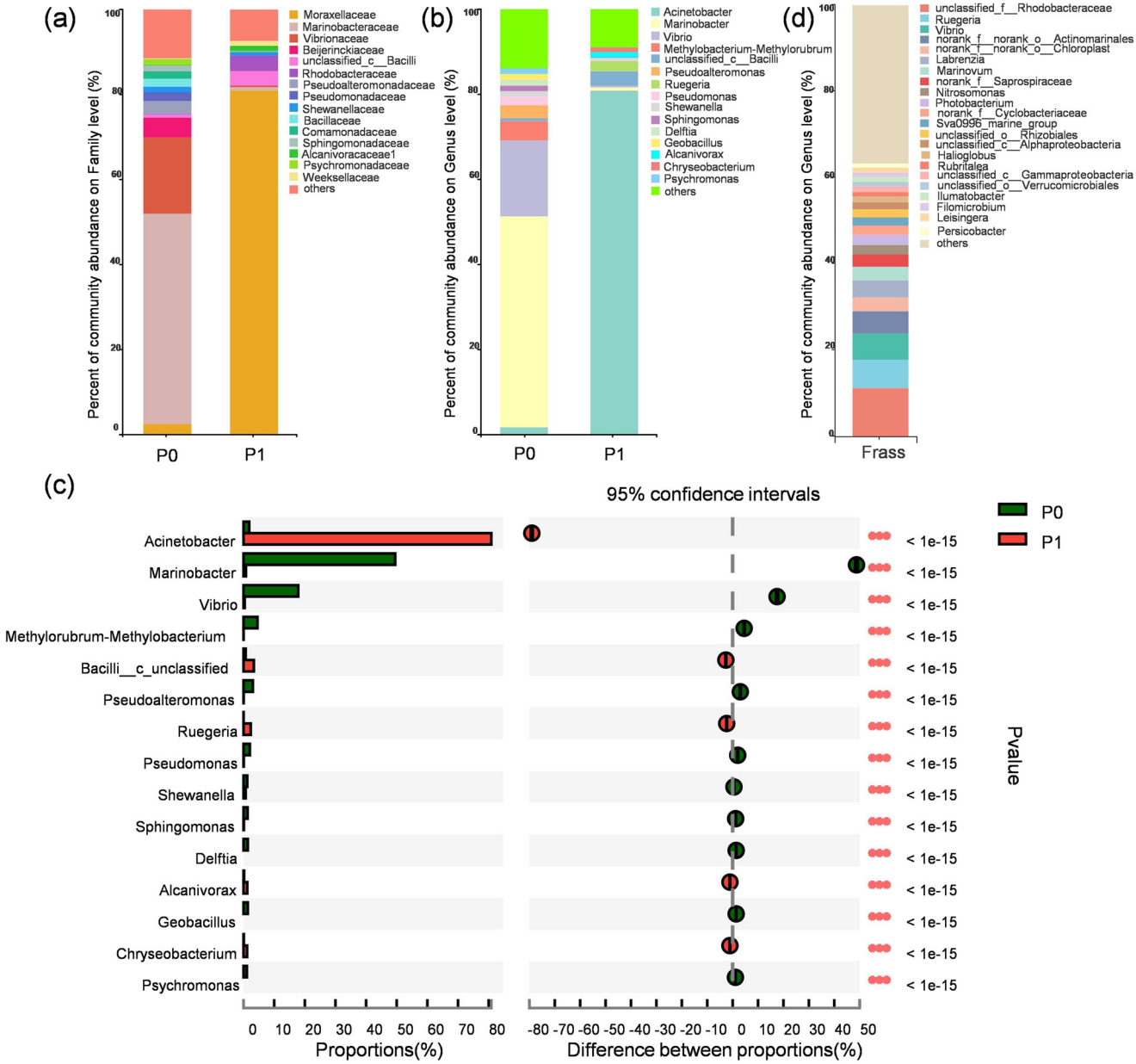

Fig. 4 | Changes of the gut microbial community of *P. vancaurica* after feeding EPS. a Column diagram of bacterial percent of gut flora microbial community of *P. vancaurica* at the family level. **b** Column diagram of bacterial percent of gut flora microbial community of *P. vancaurica* at genus level. **c** Discriminant analysis of genus abundance difference between the nonplastic-fed group (P0) and the EPS-fed group (P1). **d** Column diagram of bacterial percent of frass flora at genus level.

microplastics and increase the negative effects of EPS blocks. Thus, the plastic chewing and eating behaviours of *P. vancaurica* generate microplastics that may amplify endocrine disruption and other toxic effects on marine animals by releasing plastic additives and/or adsorbing other environmental chemicals[33]. Plastic-eating polychaetes are also at the lower end of the marine animal food chain and can be consumed by fish, shrimp and crabs, thus bringing microplastics into the food chain. In the future, the laboratory feeding conditions of clamworms should be optimized for sustained biodegradation of EPS, and further studies should be carried out to investigate the EPS bioconsumption rate.

Gut bacterial diversity specialization for EPS consumption

To explore the effect of a plastic diet on the gut microbiome, we sequenced bacterial 16 S rRNA genes from the guts of clamworms from both the plastic-fed (P1) and nonplastic-fed (P0) groups. Sequencing revealed differences in the diversity of the clamworm gut microbiome between the two groups. The results showed that in the nonplastic-fed gut microbiome, the dominant members were affiliated with *Marinobacteraceae* (49.51%), *Vibrionaceae* (17.92%), *Beijerinckiaceae* (4.68%), and *Pseudoalteromonadaceae* (3.03%) at the family level (Fig. 4a). In contrast, the EPS-fed group was dominated by the family *Moraxellaceae* (80.98%), in addition to the presence of *Rhodobacteraceae* (3.60%) and unclassified_c_*Bacilli* (3.40%). The *Marinobacteraceae* and *Vibrionaceae*, which were dominant in the nonplastic-fed group, only exhibited very low abundances—0.78% and 0.39%, respectively—in the plastic group (Fig. 4a).

At the genus level (Fig. 4b), in the nonplastic-fed group, the dominant members were *Marinobacter* (49.5%), *Vibrio* (17.8%), *Acinetobacter* (1.8%), and *Pseudoalteromonas* (3%). However, after fifteen days of EPS feeding, the plastic-fed group was dominated by the genus *Acinetobacter* (80.8%), which belongs to *Moraxellaceae*, in addition to *Ruegeria* (2.3%) of *Rhodobacteraceae*, unclassified_c_*Bacilli* (3.3%), *Chryseobacterium* (1.1%), *Alcanivorax* (1.2%), and *Vibrio* (0.38%).

The gut bacterial diversity was further compared using the chi-square test (two-tailed test) with multiple validation-corrected P values. Confidence intervals were calculated using the "Diff Between Prop Asymptotic CC" CI method with a confidence level of 0.95. Compared with animal feed consumption, EPS consumption caused a shift in the relative abundance of the genera *Acinetobacter*, *Ruegeria*, and unclassified_c_*Bacilli* among the clamworm gut microbes (Fig. 4c). In addition, to observe the microbial diversity in clamworm frass in vitro, DNA was extracted from the frass in the clamworm holes for 16 S rRNA gene sequencing. The bacterial diversity at the genus level showed that the predominant *Acinetobacter* species in the gut disappeared from this environment, as did the unclassified_*Bacilli* (3.3%). Instead, the bacteria associated with the frass in vitro were dominated by unclassified_f_*Rhodobacteraceae* (11.8%), *Ruegeria* (6.8%), *Vibrio* (4.6%), norank-*Chloroplast* (6.2%), and norank-Actinomarinales (5.2%) (Fig. 4d), which may promote further degradation of EPS outside of the clamworm.

A comparison of *G. mellonella, T. molitor*, *Z. atratus*, *T. obscurus*, *A. fulica* and *P. davidis* revealed that PS feeding led to an increase in the abundance of *Enterococcus* and Enterobacteriaceae, indicating that these genera are associated with PS degradation[15,16,28,29,31,34–37]. Other bacterial genera closely associated with PS degradation include *Bacillus* and *Serratia*, which were isolated from the gut of *G. mellonella*; *Serratia*, *Exiguobacterium*, *Citrobacter*, *Klebsiella*, *Pseudomonas*, *Bacillus*, *Lactococcus* and *Cronobacter*, which were isolated from the gut of *T. molitor*; *Pseudomonas*, *Lactococcus*, *Kluyvera*, *Acinetobacter* and *Sphingobacterium*, which were isolated from the gut of *Z. atratus*; and *Lactococcus* and *Serratia*, which were isolated from the gut of *P. davidis*[29,31]. In contrast, the genera *Enterococcus*, *Serratia*, *Pseudomonas* and *Lactococcus* commonly reported in previous studies were not found in the gut of our clamworms; instead, the genera *Acinetobacter* and *Bacilli* dominated as potential PS degraders. Both have been reported to be involved in plastic biodegradation[31]. For example, an increase in *Acinetobacter* abundance was observed during the progression of PS feeding by *T. castaneum* larvae, in addition to an increase in *Enterococcus* abundance[14].

These results suggest that the ingestion of EPS by clamworms leads to changes in the gut microbiome, and the establishment of new microbiota is likely involved in the biodegradation of EPS by clamworms. We hypothesize that gut microbes with increased abundance after EPS feeding, such as *Acinetobacter*, *Ruegeria*, and unclassified_c_*Bacilli*, could play a role in the biodegradation of EPS in clamworm guts, although the mechanism of biodegradation needs further investigation.

In previous studies, PAHs could be transformed in another clamworm, *Perinereis aibuhitensis*, by metabolic enzymes (cytochrome P450 enzymes (CYPs) and glutathione S-transferases (GSTs)), and the increase in the GST enzyme under xenobiotic exposure in *P. aibuhitensis* suggested the role of GST in detoxification and biotransformation[38]. From the digestive tract of *P. aibuhitensis*, diesel-utilizing bacterial strains of *Pseudomonas* and *Vibrio* have been isolated[39]. In these studies, *P. aibuhitensis* were collected at low tide and then temporarily reared in sterile seawater for direct isolation of gut microorganisms or with in situ sediment and seawater for long-term domestication, which required strict management of aeration, water temperature, salinity, photoperiod, and feeding with commercially formulated diets during domestication and subsequent experiments[38,39]. In the future, we also need to further explore the EPS-feeding conditions in the laboratory to verify the degradation ability of *P. vancaurica* and the specific contribution of gut microbes to EPS degradation, as well as additional studies on other species of *Perinereis* and their gut microbes in different geographic locations to determine the ubiquity of plastic degradation.

Identification of PS-degrading microorganisms in the gut

To characterize additional heterotrophic gut bacteria that may contribute to EPS digestion in clamworms, intestinal bacteria were isolated via two agar media and further characterized. Consequently, a total of 28 bacterial strains were isolated (Supplementary Table S3). Molecular characterization of the 16S rRNA gene sequences revealed that the bacteria belonged to *Gammaproteobacteria*, *Alphaproteobacteria*, *Actinomycetia*, *Flavobacteriia*, *Sphingobacteriia*, and *Bacilli*. Among *Gammaproteobacteria*, most bacteria belonged to the genera *Acinetobacter* and *Vibrio*, whereas the others belonged to the genera *Litorilituus*, *Marinobacterium*, *Photobacterium*, *Pseudoalteromonas*, *Pseudomonas*, and *Shewanella*.

To verify the PS degradation ability of the strains, each isolate was inoculated into MMC liquid media supplemented with PS films. After 30 days of incubation, ten isolates were positive for PS degradation; these isolates were *Acinetobacter* (three strains), *Brevibacterium* (one strain), *Gaetbulibacter* (three strains), *Ruegeria* (two strains), and *Vibrio* (one strain). The most effective degraders were *A. johnsonii, B. casei*, and *R. arenilitoris*, which were designated M1-3, R3-1D, and M3-42, respectively. These strains are most closely related to *A. johnsonii* ATCC 17909^T, *B. casei* ATCC 35513^T, and *R. arenilitoris* KCTC 23960^T, with similarities of 99.34%, 99.14%, and 99.98%, respectively. The phylogenetic tree of the three bacterial species based on the NJ method using the 16S rRNA gene sequences is shown in Supplementary Fig. S6. *Acinetobacter* is also enriched in the gut of *T. castaneum* through PS feeding; furthermore, the isolate *Acinetobacter* sp. AnTc-1 can degrade PS[14]. Recently, a strain of *A. johnsonii* JNU01 was isolated from soil and confirmed to degrade PS[40]. In vitro culture of the gut from *G. mellonella*, *T. obscurus* and *Z. atratus* larvae previously fed PE led to the isolation of *Acinetobacter* spp. However, *Acinetobacter* sp. strain NyZ450 and *Bacillus* sp. strain NyZ451 were isolated from the yellow mealworm *T. molitor*, and coculture assays exhibited better results for PE biodegradation[41].

Acinetobacter species have been confirmed to degrade a variety of organic pollutants, such as alkanes, polycyclic aromatic hydrocarbons, creosotes[42], and 4-hydroxybenzoic acid[43]. Thus, *Acinetobacter* species are often found in activated sludge, sewage, creosote-polluted groundwater, and oil-contaminated soil[44–46]. *Acinetobacter* species are highly adaptable to various environments, partially because of their genomic plasticity and open pangenome[47], and their adaptation to the invertebrate gut for PS consumption and degradation requires further investigation. In addition to *Acinetobacter*, both gut bacterial 16 S rRNA gene sequencing and isolation revealed that the isolates *B. casei* R3-1D and *R. arenilitoris* M3-42 were active in PS. The *Ruegeria* genus belongs to the Roseobacter clade and is frequently isolated from marine environments[48–50], and these bacteria have been reported to be n-alkane degraders and found in relatively high abundance on the surface of microplastics[5,51,52]. To the best of our knowledge, *R. arenilitoris* M3-42 was the first identified *Ruegeria* species to degrade PS. Members of the *Brevibacterium* genus are diverse and widespread in marine environments, though they are not as predominant as the other two bacteria (Fig. 4b). Consistently, a gut isolate of *Brevibacterium* from superworm (*Z. atratus*) larvae was recently confirmed to degrade PS[36].

We selected *A. johnsonii* M1-3, *B. casei* R3-1D, and *R. arenilitoris* M3-42 for further investigations. These species were deposited in the Marine Culture Collection of China (MCCC) under the accession numbers 1A18346, 1A1836, and 1A18356; their corresponding GenBank accession numbers of the partial 16S rRNA gene sequence are 0P854692, 0P854691, and 0P854690, respectively.

PS film biodegradation caused by the activity of the three bacteria

SEM analysis was performed to observe whether the PS surface was coated with bacteria. After incubating each strain with the PS film for 30 days, a piece of plastic was randomly selected for observation under SEM. As shown in Fig. S7, a large number of bacterial cells attached to the surface of the PS film formed a dense biofilm (Supplementary Fig. S7a). The attachment of bacteria to a plastic surface is the first step in carrying out subsequent biodegradation[53]. The viability of the bacteria attached to the biofilm was measured using a fluorescence microscope after staining. A large number of living cells (green) colonized the PS plastic film as biofilms (Supplementary Fig. S7c). At the colonizing sites, the surface of the PS films showed many cavities and pits, indicating that bacterium-induced PS degradation and fragmentation were underway (Supplementary Fig. S7b). In the parallel control without bacterial inoculation (CK), the surface of PS film remained smooth, and no morphological alterations were observed.

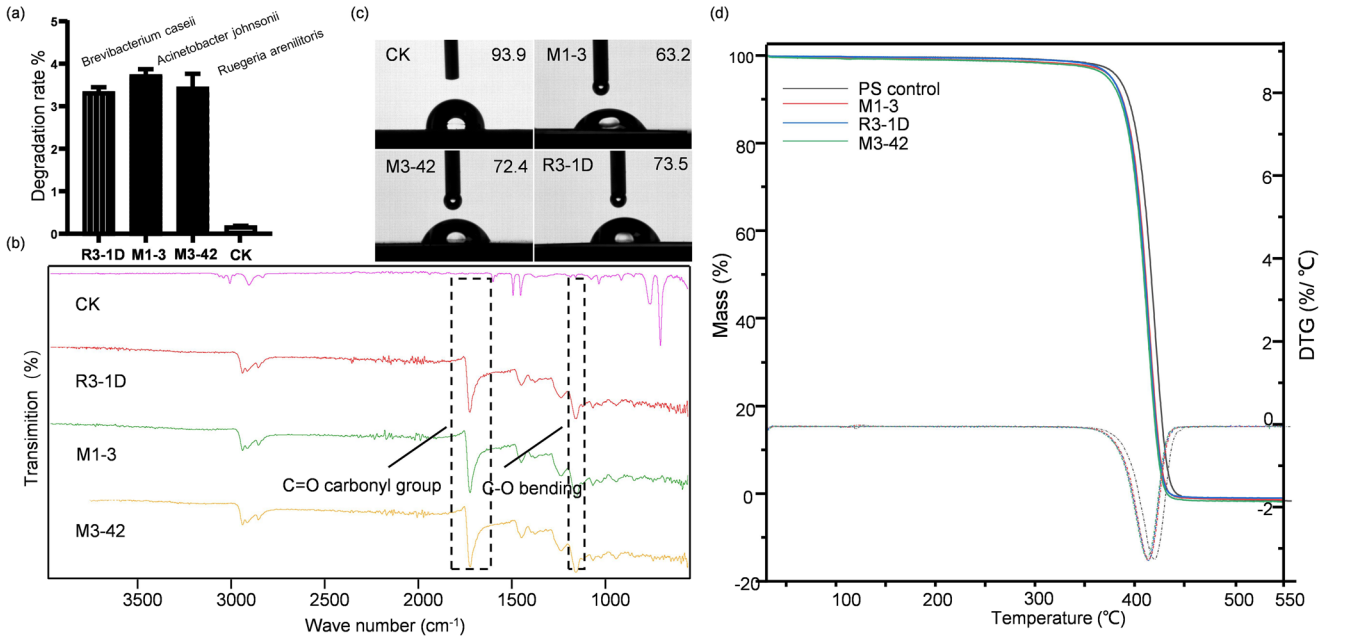

Fig. 5 | PS depolymerization and degradation intermediates by the gut bacterial isolates *B. casei* R3-1D, *R. arenilitoris* M3-42 and *A. johnsonii* M1-3. a PS weight loss after incubation with three gut bacterial isolates in 30 days (mean value ± SD, $n = 3$). **b** FTIR analysis of degraded polystyrene showed surface chemical modifications, (CK) non-inoculated PS, (M1-3) (M3-42) (R3-1D) corresponding strains incubated PS had a increase in the number of peaks in the black curved box area. **c** WCA values of (CK) the negative control PS film ($n = 3$) and (M1-3, M3-42 and R3-1D) the biodegraded PS film by the isolated three bacteria ($n = 3$). **d** After the incubation of three strains, the PS thermal stability decreased compared to the control.

To evaluate the degradation capacity of these bacterial species, the weight loss of the PS was measured after 30 days of incubation. Initial plastic weights of 3.7 ± 0.07%, 3.3 ± 0.06%, and 3.4 ± 0.18% were lost by the degradation of the gut isolates *A. johnsonii* M1-3, *B. casei* R3-1D, and *R. arenilitoris* M3-42, respectively, in the control treatment, with a final weight of 0.015 ± 0.003% (Fig. 5a). The reduction in the PS film weight suggested that the three strains can degrade and utilize PS as the sole carbon and energy source. Comparatively, our three isolates showed weaker degradation at 30 days, while the terrestrial gut isolates *Acinetobacter* sp. AnTc-1 and *Exiguobacterium* sp. YT2 resulted in 12.14 ± 1.4% and 7.4%, respectively, of the weight loss of PS after 60 days. This difference may be attributed to the variations in the PS materials used, culture media and conditions[12,14]. However, their contribution to EPS digestion in marine hosts is undoubtedly due to their dominance in the gut microbiome of the clamworm.

Changes in the chemical functional groups of the PS plastic after biooxidation were studied using FTIR analysis (Fig. 5b). The plastic films degraded by the strains M1-3 (CI = 18.33), M3-42 (CI = 24.17), and R3-1D (CI = 20.6) showed new absorption peaks at 1725 cm^{-1} in comparison to the PS control (CI = 1.55), which represents the carbonyl (C=O stretch) group. The peak at 1060 cm^{-1} represents C-O stretching, which implied the formation of a new ester or carboxylic acid from the degradation of the PS polymer. The presence of carboxyl and carboxylic acid groups is considered to be an essential step in the oxidation and biodegradation of PS[54].

The change in hydrophobicity of the washed PS film after bacterial incubation can also indicate chemical alteration. After incubation with the M1-3, M3-42, or R3-1D strains, the WCA was significantly lower ($P < 0.005$; Student's t test) than that of the control group (93.9° ± 0.2), by 63.2° ± 0.4, 72.4° ± 0.2, or 73.5° ± 0.2 ($n = 3$), respectively (Fig. 5c). The PS surface became more hydrophilic due to the generation of polar functional groups by these strains, which further increased the susceptibility of the PS to further degradation. The thermal stabilities of the PS films were examined using TGA. In comparison with the endothermic temperature of the PS control at 421 °C, the bacterially treated PS films (Fig. 5d) had a lower endothermic temperature at 413 °C–414 °C, indicating that the PS control was relatively thermally stable and that a composition change occurred in the bacteria-treated PS. Diverse gut bacterial isolates showed PS-degrading potential, which extended the diversity of PS-degrading bacteria and provided insights into the interactions of marine benthic invertebrates with plastic-degrading bacteria in association with EPS contaminants.

PS degradation intermediates of the three gut bacteria indicated by GC–MS

To confirm the occurrence of PS biodegradation by the three gut isolates M1-3, R3-1D, and M3-42, the metabolites of PS biodegradation and the medium from the control group (CK) were analyzed using GC-MS. The degradation products of the three strains all contained benzene ring substances, unlike those of the control, including diverse PS monomers (blocks) in the form of ethylbenzene (peak 2), o-xylene (peak 3), benzaldehyde (peak 4), 4-phenylbut-3-ene-1-yne (peak 5), butylated hydroxytoluene (peak 14), 3-butynylbenzene (peak 15), pentanoic acid, 2-phenylethyl ester (peak 16), and 1,2-benzene dicarboxylic acid, butyl-m (peak 17). Apart from the identified PS oligomers, fatty acids and fatty acid esters were identified in the degradation products, including butanoic acid (peak 1); carbonic acid; dodecyl prop-1-en-2-yl ester (peak 7); and methoxyacetic acid, 2-tetradecyl ester (peak 8). The remaining intermediates were hydrocarbons and alcohols, including decane, 2,3,5,8-tetramethyl- (peak 6); nonadecane, 2,3-dimethyl- (peak 9); 2-butyl-1-octanol (peak 10); 2-isopropyl-5-methyl-1-heptanol (peak 11); tetradecane (peak 12); and eicosane, 2-methyl- (peak 13). A representative scheme of the identified PS monomers and substances resulting from their degradation/reaction is presented in Supplementary Fig. S8 and Supplementary Table S4.

In our study, PS oligomers, fatty acids, and fatty acid esters were structurally similar to the extracted metabolites of frass, intestine tissue, and biomass of *G. mellonella* and *T. molitor* larvae of PS-feeding treatments[13,16,24–26]. The substances identified in the above studies were similar in structure to the individual bacterial PS degradation products, including styrene (C_8H_8) and ethylbenzene (C_8H_{10}) (peak 2), α-methyl styrene (C_9H_{10}) and o-xylene (C_8H_{10}) (peak 3), acetophenone (C_8H_8O) and benzaldehyde (C_7H_6O) (peak 4), and 2,4-di-tert butyl phenol ($C_{14}H_{22}O$) and butylated hydroxytoluene ($C_{15}H_{24}O$) (peak 14). Hexadecanoic acid, methyl ester ($C_{17}H_{34}O_2$) and 4-methyl-2,6-ditert-pentylphenol ($C_{16}H_{26}O$)

in the gut of EPS-fed clamworms were structurally similar to methoxyacetic acid, 2-tetradecyl ester ($C_{17}H_{34}O_3$) and butylated hydroxytoluene ($C_{15}H_{24}O$) in the PS metabolites of our three gut isolates, respectively, which reconfirmed that gut microbes play an important role in EPS degradation. The formation of benzaldehyde (peak 4)[55] and 2-isopropyl-5-methyl-1-heptanol (peak 11)[56] in this study was previously reported and likely occurred from chain depolymerization and oxidation of PS. Potential metabolic pathways involving PS in the gut of plastic-feeding insects have been proposed previously. In this study, the styrene oxide-phenylacetaldehyde pathway was validated by the positive detection of corresponding metabolites, such as benzaldehyde, ethylbenzene and pentanoic acid, 2-phenylethyl ester[13,26]. In summary, our results are consistent with previous reports on PS metabolic pathways based on degradation products.

However, the presence of butanoic acid in the PS metabolite of the *B. casei* R3-1D strain has not been previously reported. Butyric acid is the main energy substrate for colonocytes and stimulates the absorption of sodium and water in the colon[57]. We speculated that interactions between the bacterium *B. casei* and the host *P. vancaurica* occur during the PS digestion process. In summary, the presence of low-molecular-weight oligomers and other metabolites strongly supports PS biodegradation by gut bacteria in vitro.

Although gut microbes and clamworms have been confirmed to be involved in the biodegradation of plastics, the specific enzymes involved in the degradation of EPS by host-secreted bacteria and gut bacterial isolates have not yet been identified. The contributions of specific physicochemical processes during insect chewing and digestion may also contribute to EPS biodegradation in the host[58]. The multienzyme system and other detoxification pathways used by the host to address oxidative stress may play a role in the detoxification of depolymerization products and plastic additives[59–61]. In the future, degradative enzymes from gut bacteria and clamworms could be explored for use in bioengineering the degradation of PS.

Conclusion

To the best of our knowledge, we reported the first EPS-eating marine benthic polychaete *P. vancaurica* and its gut microbiome involved in PS biodegradation. EPS was fragmented into MPs through ingestion and biodegradation in the gut. This biological process is notable considering the prevalence of clamworms in marine environments and their close association with EPS. EPS biodegradation, at least partially, within the clamworm gut is attributed to the activity of the gut microbiome, as *Acinetobacter, Ruegeria*, and other potential degraders were enriched in the gut of clamworms fed EPS, with *Acinetobacter* being the predominant member. The microbial-mediated degradation of the strains was reconfirmed with pure cultures of the gut isolates of *A. johnsonii*, *B. casei*, and *R. arenilitoris*. The formation of degradation products and changes in physical and chemical properties were observed in response to the PS bacterial treatments, in addition to a weight loss of 3.3–3.7% in 30 days, although these values are lower than those for the terrestrial larval gut isolates of *T. molitor* and *T. castaneum*. Overall, the boring and plastic chewing behaviour of the clamworm contributes to EPS fragmentation and biodegradation, possibly causing microplastic accumulation in marine ecosystems, and the specialized microbiome of the clamworm gut has a capacity for PS degradation in vitro.

Materials and methods

EPS plastic foam and clamworm sampling

Dense mariculture, such as oyster aquaculture, has developed for several decades along the west coast of the Taiwan Strait and the coastline in China. EPS is widely used in mariculture as a buoyant material, and microplastics have been reported to exist along the strait[10,62–66]. The collection site was located on the east coast of Xiamen Island, China (118°.20′ E, 24°.49′ N), where broken EPS floating devices used in mariculture were pounded by waves on the beach at high tide and collected at low tide (Supplementary Fig. S1). EPS blocks with visible holes on the surface for clamworms to crawl through were selected, placed in disposable bags, and brought back to the laboratory. After collecting three samples in September 2021, the EPS blocks were disintegrated using scissors, and a group of clamworms was removed from the smaller EPS blocks with forceps in the lab immediately. We found approximately twenty clamworms (length 5-12 cm) living inside the EPS, chewing on the EPS, and forming tunnels filled with brown frass (Fig. 1). The original EPS around the clamworm tunnels was preserved in the dark as an EPS control for subsequent experiments.

To determine the phylogenetic position of the clamworm, 0.02 g of muscle tissue from the tail of the clamworm was excised and crushed in sterile potassium phosphate buffer (pH 7). DNA was extracted using a marine animal DNA column extraction kit (BTN130401, Co. Beijing Baiao Leibo Technology, Ltd., China). The mitochondrial-based cytochrome C oxidase subunit I (COI) and mitochondrial 16 S rRNA gene sequences commonly used for genetic diversity and genetic structure analysis of *Perinereis* species were amplified using the primers listed in Table S1 (Supporting Information). To construct the phylogenetic tree (MEGA-7), the mitochondrial 16 S rRNA gene sequences of clamworms and their relatives were retrieved from the National Centre for Biotechnology Information (NCBI, http://www.ncbi.nlm.nih.gov/) and aligned using ClustalW[67]. We used a stereomicroscope (Leica M80) to observe the morphological features of the clamworms.

To obtain the best view and clarity of the clamworm placed on the carrier stage, the eyepiece, magnification and light source of the stereomicroscope were adjusted.

Microscopy and size analysis of the EPS frass excreted by clamworms

0.2 g of excreted frass and EPS control were digested using 10% KOH solution (24 h, 50 °C) followed by H_2O_2 (24 h, 50 °C), and filtered as described in Supplementary Note S1 for subsequent analysis of particle size and chemical component changes. The size and the morphology of EPS microplastics in the clamworm frass were observed under a stereomicroscope (M205A, Leica, German), light microscope (80i, Nikon, German) and scanning electron microscopy (SEM) (LEO-1530, Germany)[68]. Detailed procedures for observing frass using a stereomicroscope were described in Supplementary note S2. EPS debris in the gut were observed using a stereomicroscope (LEICA M80), followed by observation of the surface biofilms using an all-in-one fluorescent microscope (BZ-X810, Keyence) after stained with the LIVE/DEAD BacLight Bacterial Viability Kit (USA).

Changes in the chemical properties of EPS debris in the intestine and the excreted frass

Clamworm individuals were randomly selected and immersed in 75% ethanol for 1 min and then washed with filtered seawater (0.22μm, Millex-GP) three times to remove bacteria and frass attached to the body surface. Clamworm guts, mainly the intestine, were removed with a sterile scalpel, scissors, and forceps. To obtain the degradation products of EPS in the gut, gas chromatography-mass spectrometry (GC-MS) analysis was subsequently performed on the intestine and fresh frass. Briefly, 0.05 g of fresh brown frass in parallel with EPS test control was extracted with 5 mL tetrahydrofuran (THF) and the intestines of five clamworms were extracted with 5 mL THF: methanol (2:1)[16]. Evaporated the solvent and then redissolved in 1 mL 100% hexane for GC-MS analysis. GC-MS was performed using an Agilent GC/MS-QP2010 with a DB-5MS UI (60 m × 0.25 mm × 0.25 μm) column with helium as the carrier gas. The oven temperature started at 50 °C and increased to 250 °C at a rate of 10 °C/min, and a 20-minute hold. Compounds were identified using the NIST14 database and selected for ≥70% similarity.

The cleaned clamworms and EPS test control were processed using the same digestion and filtration methods as previously described in Supplementary note S1. To observe whether the functional group of the EPS had been altered in the gut, we used micro-Fourier transform infrared spectroscopy (μFTIR: Nicolet iN10, Thermo Fisher Scientific) to discern EPS

fragments in the gut. Through 16 scans, the spectral with a range of 670-4000 cm^{-1} and a resolution of 8 cm^{-1} was obtained. In this study, the carbonyl index (CI) and hydroxyl index (HI) were used to assess the degree of oxidation on the surface of EPS debris in the gut, which were calculated as a ratio of carbonyl band area and hydroxyl group band area to methylene peak area, respectively, as reference described[69,70].

The digested frass and the EPS control were analyzed using FTIR (Nicolet iS50, Thermo Fisher Scientific, USA). The molecular weight distribution (MWD), weight-average molecular weight (Mw) and number-average molecular weight (Mn) of the EPS were tested by Gel permeation chromatography (GPC) (Agilent 1260 Infinity II, Agilent Technologies Inc., USA) with a flow rate of 0.7 mL/min using THF (1 $g{\cdot}L^{-1}$) as a solvent[28]. The MWD calculation and presentation methods are described in the relevant literature[29]. Polymer dispersity index (PDI) is a polymer dispersion index used to describe the molecular weight distribution of a polymer. Polydispersity Index (PDI) was calculated as PDI = Mw/Mn[71]. Proton nuclear magnetic resonance (^{1}H NMR) (Avance, Bruker, Germany) spectroscopy was conducted at 400 MHz to analyze the altered chemical composition of frass. The 20 mg frass was dissolved in deuterated chloroform (purity ≥99.9%)[34].

Gut microbiome analysis

Samples were divided into two groups. In the nonplastic-fed group (P0), the clamworms (5-20 cm) were purchased from fishing shops nearby the sampling site where they were artificially fed with animal feed containing fish and soybean meal, whereas in the EPS-diet group (P1), small blocks of EPS, that contained clamworm (5-12 cm), were broken down from the EPS from at sampling site using scissors and forceps and placed in plastic containers with filtered seawater (0.22um, Millex-GP) at room temperature for 15 days. The animal intestines were acquired using the same methods as previously described. The analysis procedures for bacterial community structures are described in Supplementary note S3.

Isolation and identification of PS-degrading microorganisms from the clamworm gut

To obtain more heterotrophic bacteria in the gut of the clamworms for later validation experiments of PS degradation, the gradient dilution of ground intestinal tissue solution was spread on Marine Broth 2216 and R_2A (BD Difco) agar plates. The isolation of strains and the building of phylogenetic trees were detailed in Supplementary note S4. To assess the utilization of PS by different strains, individual strains were inoculated into 50 mL liquid carbon free mineral medium (MMC) for preliminary screening, which contained three (1 × 1 cm) sterile PS films (GF94795701, thickness 0.19 mm, size 150 × 150 mm, purity ≥99.9%, Sigma, USA) as the sole carbon at 28 °C for 30 days (150 rpm/min) in the dark. All PS films used in this study were treated with 75% ethanol and rinsed three times with sterile water and dried at 50 °C for two hours. The composition of MMC is described in the literature[68]. The mineral medium was autoclaved at 121 °C for 20 min. The PS films were added as a control (CK) to the MMC liquid medium without bacteria inoculation. Bacterial growth was evaluated by biomass and cell density was re-examined under light microscope. The composition of the medium is described in the reference[68]. The same culture conditions were used for all subsequent PS degradation validation experiments. Out of 28 marine bacterial isolates, three isolates (M1-3, R3-1D, and M3-42) were found promising for PS degradation during screening.

Characterization of biodegradation of PS film by isolated gut bacteria

The degradation defects and biofilm of the isolated strains on the PS surface were observed using SEM (LEO-1530, Germany), as described previously by Zhao et al.[68]. After 30 days of inoculation of the strains *A. johnsonii* M1-3, *B. casei* R3-1D, and *R. arenilitoris* M3-42, respectively, PS films were randomly removed from the culture. To analyze changes on the PS surface after bacterial degradation, 2% w/v sodium dodecyl sulfate (SDS) solution was used to remove the bacteria attached to PS films incubated for 4 h at 50 °C, then washed with sterile ddH_2O to remove SDS and then dried at room temperature[29]. The remaining washed PS films were used for the experiments below. To determine the bacterial survival status on PS films, the biofilm on PS films was stained with the LIVE/DEAD BacLight Bacterial Viability Kit (USA), after washing with MMC liquid medium to remove the free-living cells[72]. Finally, the PS films were observed using a fluorescent microscope (Nikon 80i). The control (CK) was three pieces of PS film in MMC liquid medium without bacterial inoculation, in parallel with bacterial treatments from medium preparation to incubation and observation.

To determine PS degradation by the pure gut bacteria, the PS weight loss was measured after 30 days of incubation in flasks loaded with 50 mL of MMC at an initial pure bacterial cell density of 0.5. The reduction of the weight of PS was measured as described previously by Liu et al.[72]. The PS films (CK) were also treated using the same procedure. Weight loss was calculated using Ref's formula[73]. Percentage of weight loss = 100 × [(Initial PS weight − Final PS weight)/Initial PS weight].

The altered chemical structure of the PS surface was characterized using an infrared spectrometer (Thermo Scientific iS50, USA) operating in attenuated total reflection (ATR) mode for FTIR analysis. After drying, bacteria-treated PS films and CK were recorded and spectra across 500–4000 cm^{-1} were acquired with a spectral resolution of 4 cm^{-1} over an average of 32 scans using OMSNIC software. The water contact angle (WCA) (OCA20, Dataphysics, Germany) was used to characterize the change in PS surface hydrophilicity after degradation. To measure the WCAs, distilled water (2 μL) was dropped on dried PS films at 2 μL/s. The WCAs were calculated using the SCA20 software and averaged over three replicated measurements[29]. The change in thermal stability of bacteria-treated PS films compared to the CK was measured using thermogravimetric analysis (TGA) (TGA 2, Mettler Toledo, USA). Samples were heated from 30 to 550 °C at a rate of 10 °C /min under a high-purity nitrogen ambience[35].

Analysis of PS-degradation intermediates with GC–MS

GC–MS was performed to investigate the intermediate and end products of plastic biodegradation by M1-3, R3-1D, and M3-42. After 30 days of incubation with 3 (1 × 1 cm) sterile PS films in Erlenmeyer flasks, 50 ml liquid culture of three different strains was centrifuged (8000 rpm/min, 10 min, 4°C) and 0.22-μm filtered (Millex-GP) to obtain the supernatant. Then supernatant was extracted three times with 50 mL chloroform: methanol (v: v, 2:1)[24]. The solvent was evaporated and then redissolved in 1 mL 100% hexane. The same medium without bacterial inoculation was used as a control group (CK), in parallel with bacterial treatments from medium preparation, cultivation and extraction. As with the analysis of degradation products of EPS in the gut, the GC-MS analysis followed the same procedure.

Reporting summary

Further information on research design is available in the Nature Portfolio Reporting Summary linked to this article.

Data availability

Raw sequencing reads for bacterial diversity analysis have been deposited at Genome Sequence Archive (https://ngdc.cncb.ac.cn/gsa/) (accession numbers: CRA010201).

Code availability

No custom code was developed for the results in this manuscript.

Supplementary Information

Tables (S1–S4) on information of primers for the PCR amplification of COI and mitochondrial 16S rRNA gene, identified compounds in the extract of intestine and frass resulting from biodegradation of EPS by clamworm, isolation and characterization of PS-degrading bacteria from the gut of *Perinereis vancaurica*, identified compounds in the extract of the culture supernatants resulting from biodegradation of PS by isolated strains. Figures (S1–S8) on information of map of the sampling site, stereo

micrograph of *P. vancaurica*, phylogenetic relationships of *P. vancaurica*, observation of the biofilm on the surface of EPS debris in the intestine, light micrograph of the particle size of EPS frass, phylogenetic tree of PS-degrading bacteria, SEM images of the biodegraded PS film by the isolated bacterium, and GC-MS analysis of the culture supernatant with isolated strains and control group (CK). Note (S1-S4) on information of procedures of digestion, for observing frass, sequencing bacterial community structure, isolation of strains and establishment of phylogenetic trees.

Received: 27 October 2023; Accepted: 12 March 2024;
Published online: 28 March 2024

References

1. PlasticsEurope2022. Plastics-the facts 2022; https://plasticseurope.org/knowledge-hub/plastics-the-facts-2022-FINAL-for-website.pdf.
2. Kaiser, J. The dirt on ocean garbage patches. *Science* **328**, 1506 (2010).
3. Liu, P. S.; Chen, G. F., Chapter Eight - Applications of Polymer Foams. In *Porous Materials*, Butterworth-Heinemann: Boston; pp 383–410. 2014.
4. Wang, L. et al. Environmental fate, toxicity and risk management strategies of nanoplastics in the environment: Current status and future perspectives. *J. Hazard. Mater.* **401**, 123415 (2021).
5. Zhang, Y., Lu, J., Wu, J., Wang, J. & Luo, Y. Potential risks of microplastics combined with superbugs: Enrichment of antibiotic resistant bacteria on the surface of microplastics in mariculture system. *Ecotoxicol. Environ. Saf.* **187**, 109852 (2020).
6. Turner, A. Foamed polystyrene in the marine environment: sources, additives, transport, behavior, and impacts. *Environ. Sci. Technol.* **54**, 10411–10420 (2020).
7. Thiele, C. J., Hudson, M. D., Russell, A. E., Saluveer, M. & Sidaoui-Haddad, G. Microplastics in fish and fishmeal: an emerging environmental challenge? *Sci. Rep.* **11**, 2045 (2021).
8. Lebreton, L. & Andrady, A. Future scenarios of global plastic waste generation and disposal. *Palgrave Commun.* **5**, 1–11 (2019).
9. Browne, M. A., Galloway, T. & Thompson, R. Microplastic–an emerging contaminant of potential concern? *Integr. Environ. Assess. Manag.* **3**, 559–561 (2007).
10. Pan, Z., Liu, Q., Xu, J., Li, W. & Lin, H. Microplastic contamination in seafood from Dongshan Bay in southeastern China and its health risk implication for human consumption. *Environ. Pollut.* **303**, 119163 (2022).
11. Ganesh, K. A., Anjana, K., Hinduja, M., Sujitha, K. & Dharani, G. Review on plastic wastes in marine environment - Biodegradation and biotechnological solutions. *Mar. Pollut. Bull.* **150**, 110733 (2020).
12. Yang, Y. et al. Biodegradation and mineralization of polystyrene by plastic-eating mealworms: Part 2. Role of gut microorganisms. *Environ. Sci. Technol.* **49**, 12087–12093 (2015).
13. Tsochatzis, E. et al. Gut microbiome and degradation product formation during biodegradation of expanded polystyrene by mealworm larvae under different feeding strategies. *Molecules* **26**, 7568 (2021).
14. Wang, Z., Xin, X., Shi, X. & Zhang, Y. A polystyrene-degrading *Acinetobacter* bacterium isolated from the larvae of *Tribolium castaneum*. *Sci. Total Environ.* **726**, 138564 (2020).
15. Peng, B. Y. et al. Biodegradation of polystyrene by Dark (*Tenebrio obscurus*) and Yellow (*Tenebrio molitor*) Mealworms (Coleoptera: Tenebrionidae). *Environ. Sci. Technol.* **53**, 5256–5265 (2019).
16. Lou, Y. et al. Biodegradation of polyethylene and polystyrene by greater Wax Moth Larvae (*Galleria mellonella* L.) and the effect of co-diet supplementation on the core gut microbiome. *Environ. Sci. Technol.* **54**, 2821–2831 (2020).
17. Chakraborty, A. et al. Unravelling the gut bacteriome of *Ips* (Coleoptera: Curculionidae: Scolytinae): identifying core bacterial assemblage and their ecological relevance. *Sci. Rep.* **10**, 18572 (2020).
18. Ammar el, D., Gasparich, G. E., Hall, D. G. & Hogenhout, S. A. Spiroplasma-like organisms closely associated with the gut in five leafhopper species (Hemiptera: *Cicadellidae*). *Arch Microbiol.* **193**, 35–44 (2011).
19. Vecchi, S., Bianchi, J., Scalici, M., Fabroni, F. & Tomassetti, P. Field evidence for microplastic interactions in marine benthic invertebrates. *Sci. Rep.* **11**, 20900 (2021).
20. Xi, M., Zhang, Q., Nie, L., Xiong, T. & Yu, Z. Quantitative comparison of clamworm (*Perinereis aibuhitensis*) and crab (*Macrophthalmus japonicus*) burrowing effects on nitrogen and phosphorus dynamics at the sediment-water interface. *Sci. Total Environ.* **857**, 159559 (2023).
21. Deng, Y. Molecular phylogenetic of *Perinereis* and genetic diversity analysis of *Perinereis aibuhitensis*. Master, Ocean University of China, 2014.
22. Deng, Y., Song, N., Liu, M. & Gao, T. Population genetic analysis of *Perinereis aibuhitensis* based on the mitochondrial DNA CytB. *Acta Hydrobiol. Sin.* **38**, 597–601 (2014).
23. Wang, Y. Study on taxonomy and genetic diversity of cultured *Perinereis linea* in different body colors and regions. master, Dalian Ocean University, 2022.
24. Tsochatzis, E. D., Berggreen, I. E., Nørgaard, J. V., Theodoridis, G. & Dalsgaard, T. K. Biodegradation of expanded polystyrene by mealworm larvae under different feeding strategies evaluated by metabolic profiling using GC-TOF-MS. *Chemosphere* **281**, 130840 (2021).
25. Tsochatzis, E., Lopes, J. A., Gika, H. & Theodoridis, G. Polystyrene biodegradation by *Tenebrio molitor* Larvae: Identification of generated substances using a GC-MS untargeted screening method. *Polymers* **13**, 17 (2020).
26. Wang, S. et al. Complete digestion/biodegradation of polystyrene microplastics by greater wax moth (*Galleria mellonella*) larvae: Direct in vivo evidence, gut microbiota independence, and potential metabolic pathways. *J. Hazard. Mater.* **423**, 127213 (2022).
27. Tsochatzis, E. D. et al. Cellular lipids and protein alteration during biodegradation of expanded polystyrene by mealworm larvae under different feeding conditions. *Chemosphere* **300**, 134420 (2022).
28. Song, Y. et al. Biodegradation and disintegration of expanded polystyrene by land snails *Achatina fulica*. *Sci. Total Environ.* **746**, 141289 (2020).
29. Woo, S., Song, I. & Cha, H. J. Fast and facile biodegradation of polystyrene by the gut microbial flora of *Plesiophthalmus davidis* larvae. *Appl. Environ. Microbiol.* **86**, e01361–20 (2020).
30. Yang, S. S. et al. Biodegradation of polypropylene by yellow mealworms (*Tenebrio molitor*) and superworms (*Zophobas atratus*) via gut-microbe-dependent depolymerization. *Sci. Total Environ.* **756**, 144087 (2021).
31. Pivato, A. F. et al. Hydrocarbon-based plastics: Progress and perspectives on consumption and biodegradation by insect larvae. *Chemosphere* **293**, 133600 (2022).
32. Peng, B. Y. et al. Biodegradation of low-density polyethylene and polystyrene in superworms, larvae of *Zophobas atratus* (Coleoptera: Tenebrionidae): Broad and limited extent depolymerization. *Environ. Pollut.* **266**, 115206 (2020).
33. Jiang, B. et al. Health impacts of environmental contamination of micro- and nanoplastics: a review. *Environ. Health Prev. Med.* **25**, 29 (2020).
34. Kim, H. R. et al. Biodegradation of polystyrene by *Pseudomonas* sp. isolated from the gut of superworms (Larvae of *Zophobas atratus*). *Environ. Sci. Technol.* **54**, 6987–6996 (2020).
35. Luo, L. et al. Biodegradation of foam plastics by *Zophobas atratus* larvae (Coleoptera: Tenebrionidae) associated with changes of gut digestive enzymes activities and microbiome. *Chemosphere* **282**, 131006 (2021).
36. Arunrattiyakorn, P. et al. Biodegradation of polystyrene by three bacterial strains isolated from the gut of Superworms (*Zophobas atratus* larvae). *J. Appl. Microbiol.* **132**, 2823–2831 (2022).

37. Jiang, S., Su, T., Zhao, J. & Wang, Z. Biodegradation of Polystyrene by *Tenebrio molitor*, *Galleria mellonella*, and *Zophobas atratus* larvae and comparison of their degradation effects. *Polymers* **13**, 3539 (2021).
38. Yuan, X. et al. Expression profile of a novel glutathione S-transferase gene in the marine polychaete *Perinereis aibuhitensis* in short-term responses to phenanthrene, fluoranthene, and benzo[α]pyrene. *Mar. Pollut. Bull.* **169**, 112552 (2021).
39. Wang, X., Chen, H. & Wang, B. Isolation and degradation charateristic of Oil-Degrading bacteria from the digestive tract of *Pernereis aibuhitensis*. *Environ. Dev.* **29**, 177–180 (2017).
40. Kim, H. W. et al. Biodegradation of polystyrene by bacteria from the soil in common environments. *J. Hazard. Mater.* **416**, 126239 (2021).
41. Cfya, B., Ying, X. & Nyza, B. Biodegradation of polyethylene mulching films by a co-culture of *Acinetobacter* sp. strain NyZ450 and *Bacillus* sp. strain NyZ451 isolated from Tenebrio molitor larvae - ScienceDirect. *Int. Biodeterior. Biodegradation* **155**, 105080 (2020).
42. Kaas, R. S. et al. Draft Genome sequence of *Acinetobacter johnsonii* C6, an environmental isolate engaging in interspecific metabolic interactions. *Genome Announc.* **5**, e00155–17 (2017).
43. Lu, P. et al. Biodegradation of 4-hydroxybenzoic acid by *Acinetobacter johnsonii* FZ-5 and *Klebsiella oxytoca* FZ-8 under anaerobic conditions. *Biodegradation* **33**, 17–31 (2022).
44. Fan, N., Qi, R. & Yang, M. Isolation and characterization of a virulent bacteriophage infecting *Acinetobacter johnsonii* from activated sludge. *Res. Microbiol.* **168**, 472–481 (2017).
45. Mu, X. et al. Complete genome sequence of a rare pigment-producing strain of *Acinetobacter johnsonii*, Isolated from the bile of a patient in Hangzhou, China. *Microbiol. Resour. Announc.* **11**, e0002522 (2022).
46. Lee, M., Woo, S. G. & Ten, L. N. Characterization of novel diesel-degrading strains *Acinetobacter haemolyticus* MJ01 and *Acinetobacter johnsonii* MJ4 isolated from oil-contaminated soil. *World J. Microbiol. Biotechnol.* **28**, 2057–2067 (2012).
47. Jia, J., Liu, M., Feng, L. & Wang, Z. Comparative genomic analysis reveals the evolution and environmental adaptation of *Acinetobacter johnsonii*. *Gene* **808**, 145985 (2022).
48. Roe, K. L., Hogle, S. L. & Barbeau, K. A. Utilization of heme as an iron source by marine Alphaproteobacteria in the *Roseobacter* clade. *Appl. Environ. Microbiol.* **79**, 5753–5762 (2013).
49. Rivers, A. R., Smith, C. B. & Moran, M. A. An Updated genome annotation for the model marine bacterium *Ruegeria pomeroyi* DSS-3. *Stand. Genomic Sci.* **9**, 11 (2014).
50. Sonnenschein, E. C. et al. Global occurrence and heterogeneity of the Roseobacter-clade species *Ruegeria mobilis*. *ISME J* **11**, 569–583 (2017).
51. Horiike, T. et al. Diversity of salt-tolerant tellurate-reducing bacteria in a marine environment. *J. Gen. Appl. Microbiol.* **65**, 246–253 (2019).
52. Liu, S. et al. Petroleum spill bioremediation by an indigenous constructed bacterial consortium in marine environments. *Ecotoxicol. Environ. Saf.* **241**, 113769 (2022).
53. Lucas, N. et al. Polymer biodegradation: mechanisms and estimation techniques. *Chemosphere* **73**, 429–442 (2008).
54. Masmoudi, F., Fenouillot, F., Mehri, A., Jaziri, M. & Ammar, E. Characterization and quality assessment of recycled post-consumption poly(ethylene terephthalate) (PET). *Environ. Sci. Pollut. Res. Int.* **25**, 23307–23314 (2018).
55. Du, Y. et al. Oxidative degradation of pre-oxidated polystyrene plastics by dye decolorizing peroxidases from *Thermomonospora curvata* and *Nostocaceae*. *J. Hazard. Mater.* **436**, 129265 (2022).
56. Yang, Y. et al. Mechanisms of polystyrene microplastic degradation by the microbially driven Fenton reaction. *Water Res.* **223**, 118979 (2022).
57. Manrique Vergara, D. & González Sánchez, M. E. Short chain fatty acids (butyric acid) and intestinal diseases. *Nutr. Hosp.* **34**, 58–61 (2017).
58. Goveas, L. C. et al. Microplastics occurrence, detection and removal with emphasis on insect larvae gut microbiota. *Mar. Pollut. Bull.* **188**, 114580 (2023).
59. Prokic, M. D., Radovanovic, T. B., Gavric, J. P. & Faggio, C. Ecotoxicological effects of microplastics: Examination of biomarkers, current state and future perspectives. *TrAC: Trends Anal. Chem.* **111**, 37–46 (2019).
60. Hirt, N. & Body-Malapel, M. Immunotoxicity and intestinal effects of nano- and microplastics: a review of the literature. *Part Fibre Toxicol.* **17**, 57 (2020).
61. Sanluis-Verdes, A. et al. Wax worm saliva and the enzymes therein are the key to polyethylene degradation by *Galleria mellonella*. *Nat. Commun.* **13**, 5568 (2022).
62. Wu, Q. et al. Microplastics in seawater and two sides of the Taiwan Strait: Reflection of the social-economic development. *Mar. Pollut. Bull.* **169**, 112588 (2021).
63. Tang, G. et al. Microplastics and polycyclic aromatic hydrocarbons (PAHs) in Xiamen coastal areas: Implications for anthropogenic impacts. *Sci. Total Environ.* **634**, 811–820 (2018).
64. Sun, J. et al. Microplastic pollution threats coastal resilience and sustainability in Xiamen City, China. *Mar. Pollut. Bull.* **187**, 114516 (2023).
65. Pan, Z. et al. Microplastic pollution and ecological risk assessment in an estuarine environment: The Dongshan Bay of China. *Chemosphere* **262**, 127876 (2021).
66. Long, Z. et al. Anthropocene microplastic stratigraphy of Xiamen Bay, China: A history of plastic production and waste management. *Water Res.* **226**, 119215 (2022).
67. Kumar, S., Stecher, G. & Tamura, K. MEGA7: Molecular evolutionary genetics analysis version 7.0 for bigger datasets. *Mol. Biol. Evol.* **33**, 1870–1874 (2016).
68. Zhao, S. et al. Biodegradation of polyethylene terephthalate (PET) by diverse marine bacteria in deep-sea sediments. *Environ. Microbiol.* **25**, 2719–2731 (2023).
69. Battulga, B., Kawahigashi, M. & Oyuntsetseg, B. Behavior and distribution of polystyrene foams on the shore of Tuul River in Mongolia. *Environ. Pollut.* **260**, 113979 (2020).
70. Potrykus, M. et al. Polypropylene structure alterations after 5 years of natural degradation in a waste landfill. *Sci. Total Environ.* **758**, 143649 (2021).
71. Peng, B. Y. et al. Biodegradation of Polyvinyl Chloride (PVC) in *Tenebrio molitor* (Coleoptera: Tenebrionidae) larvae. *Environ. Int.* **145**, 106106 (2020).
72. Liu, R. et al. Biodegradation of polystyrene (PS) by marine bacteria in mangrove ecosystem. *J. Hazard. Mater.* **442**, 130056 (2022).
73. Acosta-González, A., Martirani-von Abercron, S. M., Rosselló-Móra, R., Wittich, R. M. & Marqués, S. The effect of oil spills on the bacterial diversity and catabolic function in coastal sediments: a case study on the Prestige oil spill. *Environ. Sci. Pollut. Res. Int.* **22**, 15200–15214 (2015).

Acknowledgements

This work was financially supported by the Projects of the National Science Foundation of China (No. 42030412 and 91851203), Scientific Research Foundation of Third Institute of Oceanography (No. 2019021), the COMRA Program (No. DY-XZ-04 and DY135-B2-01), Xiamen Ocean Economic Innovation and Development Demonstration Project (No. 16PZP001SF16).

Author contributions

Sufang.Zhao.: Methodology; visualization; writing – original draft. Renju.Liu.: Visualization. Shiwei.Lv: Visualization. Benjuan.Zhang: Visualization. Juan.Wang: Visualization. Zongze.Shao: Conceptualization; funding acquisition; project administration; supervision; writing – review and editing.

Competing interests
The authors declare no competing interests.

Ethics declaration
Not applicable.

Additional information
Supplementary information The online version contains supplementary material available at https://doi.org/10.1038/s43247-024-01318-6.

Correspondence and requests for materials should be addressed to Zongze Shao.

Peer review information *Communications Earth & Environment* thanks Xin Zhao, Wei-Min Wu and the other, anonymous, reviewer(s) for their contribution to the peer review of this work. Primary Handling Editors: Temitope Sogbanmu and Clare Davis. A peer review file is available.